MIKAILALSYS
Journal of Multidisciplinary Sciences

e-ISSN : 2987-2286
p-ISSN : 2987-3924

Index: Harvard, Boston, Sydney, Copernicus, Sinta 4, Scilit, Semantic, Google, etc

https://doi.org/10.58578/mikailalsys.v4i3.11561

The Effect of Lemongrass Leaf and Betel Leaf Extract Ratio Variations on the Optical Characteristics and Crystal Structure of Silver Nanoparticles Synthesized via Green Synthesis

Nirmala Rahima Suci, Riri Jonuarti, Leni Aziyus Fitri, Fandi Oktasendra
Universitas Negeri Padang, Indonesia
nirmalsuci12@gmail.com

Article Info:

Submitted:	Revised:	Accepted:	Published:
Jun 14, 2026	Jul 12, 2026	Jul 24, 2026	Jul 29, 2026

Abstract

Green synthesis of silver nanoparticles (AgNPs) provides an environmentally sustainable approach by utilizing plant-derived bioactive compounds as reducing and stabilizing agents. The combination of lemongrass (*Cymbopogon citratus*) and betel leaf (*Piper betle* L.) extracts may enhance AgNP formation because both contain flavonoids, phenolic compounds, citral, eugenol, and other secondary metabolites. This study aimed to investigate the effects of different lemongrass-to-betel leaf extract ratios on the physical characteristics of AgNPs synthesized through a green synthesis method. AgNPs were prepared using extract ratios of 1:1, 3:1, and 1:3 and characterized using UV–Visible spectroscopy, particle size analysis (PSA), and X-ray diffraction (XRD). UV–Visible spectroscopy confirmed AgNP formation through surface plasmon resonance absorption bands in all samples, with maximum wavelengths of 419, 444, and 398 nm and absorbance values of 1.98, 1.98, and 2.47 for the 1:1, 3:1, and 1:3 ratios, respectively. PSA showed average particle sizes of 39.1 ± 0.9 nm, 59.7 ± 16.1 nm, and 47.2 ± 4.6 nm, with the smallest particle size obtained at the 1:1 ratio. XRD analysis confirmed that all samples possessed a face-centered cubic crystalline structure, with average crystallite sizes of 16.72 nm for the 1:1 ratio, 14.72 nm for the 3:1 ratio, and 9.37 nm for the 1:3 ratio. These findings demonstrate that variations in the composition of the dual-bioreductant system influence the optical properties, particle size, and crystallite size of the synthesized AgNPs. The 1:1 ratio produced the smallest hydrodynamic particle size, whereas the 1:3 ratio yielded the highest absorbance and smallest crystallite size. This study contributes to the optimization of plant-mediated AgNP synthesis by demonstrating that the relative composition of lemongrass and betel leaf extracts is a critical parameter for controlling nanoparticle characteristics.

Keywords: Dual Bioreductant; Green Synthesis; Plant Extract Ratio; Silver Nanoparticles; Structural Characterization

INTRODUCTION

The rapid advancement of nanotechnology has created significant opportunities for the development of materials with superior physical, chemical, and optical properties compared to their bulk counterparts. Materials with dimensions ranging from 1 to 100 nm possess a high specific surface area, resulting in enhanced reactivity, stability, and interaction efficiency with their surrounding environment. Among the various nanomaterials, silver nanoparticles (AgNPs) have attracted considerable attention due to their unique optical properties arising from the Surface Plasmon Resonance (SPR) phenomenon, stable crystal structure, and broad potential applications in biomedicine, sensing, catalysis, electronics, food packaging, and environmental remediation. Therefore, the development of efficient, environmentally friendly, and reliable methods for synthesizing AgNPs with desirable physical characteristics has become one of the major focuses of nanomaterials research (Fahim et al., 2024; Kumari & Sarkar, 2021; Rónavári et al., 2021; Sampath et al., 2022).

Silver nanoparticles can be synthesized using physical, chemical, or biological methods. Physical methods generally produce nanoparticles with high purity but require sophisticated equipment and substantial energy consumption. Chemical methods are relatively simple; however, they typically employ synthetic reducing and stabilizing agents that may generate hazardous residues. As an alternative, green synthesis utilizes plant-derived secondary metabolites as both reducing agents and capping agents. This approach is environmentally friendly, cost-effective, and consistent with the principles of green chemistry (Fahim et al., 2024; Moond et al., 2022; Mustapha et al., 2022; Vanlalveni et al., 2021).

The success of green synthesis is largely determined by the presence of plant secondary metabolites, such as flavonoids, phenolic compounds, tannins, terpenoids, alkaloids, and essential oils, which are capable of reducing Ag^{+} ions into metallic Ag^{0} while simultaneously forming a protective layer on the nanoparticle surface. Consequently, the type of plant extract used as a bioreducing agent plays a crucial role in determining the synthesis efficiency and the physicochemical characteristics of the resulting AgNPs (Mustapha et al., 2022; Pandey et al., 2025).

Lemongrass (*Cymbopogon citratus*) leaves have been widely employed as bioreducing agents because they contain citral, flavonoids, phenolic compounds, tannins, and terpenoids that facilitate both the reduction and stabilization of silver nanoparticles. Several studies have reported that lemongrass leaf extract can produce AgNPs with nanometer-scale particle sizes, a Face-Centered Cubic (FCC) crystal structure, and favorable optical characteristics as confirmed by UV–Vis spectroscopy and X-Ray Diffraction (XRD) analyses (Cherian et al., 2025; Karaiyagowder et al., 2023; Kurra, Velidandi, Sarvepalli, & Godishala, 2025; Rakib-Uz-Zaman et al., 2022). On the other hand, betel (*Piper betle*) leaves contain flavonoids, eugenol, hydroxychavicol, tannins, and phenolic compounds that function as reducing and stabilizing agents, thereby promoting nucleation and enhancing nanoparticle stability through a surface-capping mechanism (Diab et al., 2025).

Although numerous studies have reported the green synthesis of AgNPs using either lemongrass or betel leaf extracts individually, most investigations have relied on a single plant extract as the bioreducing agent. Studies combining both extracts remain limited and have primarily focused on antibacterial activity, whereas the influence of different bioreducer ratios on the optical properties, particle size, and crystal structure of AgNPs has not been systematically investigated (Diab et al., 2025; Karaiyagowder et al., 2023; Kurra, Velidandi, Sarvepalli, & Godishala, 2025). Furthermore, most previous studies have reported characterization using only one or two analytical techniques, such as UV–Vis spectroscopy or XRD. In contrast, UV–Vis spectroscopy confirms AgNP formation through the observation of SPR absorption bands, Particle Size Analyzer (PSA) provides information regarding hydrodynamic particle size and particle size distribution, while XRD is employed to determine crystal structure and crystallite size. The integration of these three characterization techniques is essential to obtain a more comprehensive understanding of the physicochemical properties of AgNPs (Fahim et al., 2024; Latumakulita, 2022; Raj et al., 2022).

The novelty of this study lies in the use of a combination of two plant extracts with varying mixing ratios as bioreducing agents, together with the comprehensive evaluation of AgNP characteristics using three complementary characterization techniques. The findings are expected to provide deeper insights into the influence of bioreducer composition on AgNP formation and to serve as a scientific basis for the development of more effective and environmentally sustainable green synthesis methods for silver nanoparticles. Therefore, this study aims to investigate the effect of varying the ratio of lemongrass (*Cymbopogon citratus*) and betel (*Piper betle*) leaf extracts as bioreducing agents on the characteristics of green-synthesized silver nanoparticles based on UV–Vis spectroscopy, X-Ray Diffraction (XRD), and Particle Size Analyzer (PSA) analyses.

METHODS

Fresh lemongrass (*Cymbopogon citratus*) and betel (*Piper betle* L.) leaves were obtained from local cultivation in Air Tawar Barat, Indonesia, in February 2026 and used as natural bioreducing agents. The chemicals used in this study included silver nitrate ($AgNO_3$) with a purity of 99.54% (Chemical Pure), supplied by PT ROFA Laboratorium Indonesia, as the precursor for silver nanoparticle synthesis. Seventy percent ethanol was used as the extraction solvent, while distilled water (aquades), obtained from PT Novalindo Jaya Utama, was used for solution preparation, sample washing, and characterization procedures.

Fresh lemongrass and betel leaves were washed thoroughly under running water and rinsed with distilled water to remove surface impurities. The samples were air-dried at room temperature (approximately 27°C), cut into smaller pieces, and further dried in a laboratory oven at 50°C for 48 h until completely dehydrated. The dried leaves were ground into fine powder using a grinder, and 100 g of each powdered sample was weighed. Extraction was carried out using the Ultrasonic-Assisted Extraction (UAE) method with 1000 mL of 70% ethanol for every 100 g of leaf powder. The mixture was sonicated at 35°C for 15 min and the extraction process was repeated three times. The resulting filtrate was separated using filter paper and concentrated with a rotary evaporator at 60°C until a concentrated extract was obtained. The extracts were stored in dark glass bottles at 4°C until further use as bioreducing agents for silver nanoparticle synthesis.

A 1 mM $AgNO_3$ solution was prepared by dissolving 8.5 mg of $AgNO_3$ in distilled water to obtain a final volume of 50 mL. The solution was homogenized using a magnetic stirrer until the $AgNO_3$ was completely dissolved and then stored in a dark bottle wrapped with aluminum foil to prevent photodegradation before use as the precursor for silver nanoparticle synthesis.

Silver nanoparticles were synthesized via the green synthesis method using a combination of lemongrass and betel leaf extracts as bioreducing agents. A total of 50 mL of 1 mM $AgNO_3$ solution was heated at 60–70°C using a hot plate magnetic stirrer. Three extract ratios were employed: 1:1 (5 mL lemongrass extract:5 mL betel leaf extract), 3:1 (7.5 mL lemongrass extract:2.5 mL betel leaf extract), and 1:3 (2.5 mL lemongrass extract:7.5 mL betel leaf extract), with a constant total extract volume of 10 mL for each treatment. The mixed extracts were added dropwise into the heated $AgNO_3$ solution while stirring continuously for 30–60 min until a homogeneous mixture was obtained. The formation of silver nanoparticles was monitored through the color change of the solution from colorless to yellowish-brown and eventually dark brown. After heating, the suspension was allowed to stand at room temperature for 12–24 h in aluminum foil-covered containers to complete the reduction of Ag^+ ions into Ag^0 and promote nanoparticle growth.

The resulting nanoparticle suspension was first characterized using UV–Vis spectroscopy to confirm nanoparticle formation based on the Surface Plasmon Resonance (SPR) absorption band. Subsequently, Particle Size Analyzer (PSA) measurements were performed to determine the average particle size and particle size distribution. After UV–Vis and PSA characterization, the nanoparticle suspension was centrifuged at 10,000 rpm for 15 min. The obtained precipitate was washed three times with distilled water and dried in an oven at 50°C to produce silver nanoparticle powder. The dried powder was stored in sealed containers wrapped with aluminum foil before characterization using X-Ray Diffraction (XRD) to identify the crystal structure and determine the crystallite size.

The UV–Vis data were analyzed based on the maximum absorption wavelength (λmax) and absorbance values to evaluate the formation of silver nanoparticles. The XRD data were analyzed according to the diffraction peak positions, Full Width at Half Maximum (FWHM) values, and crystallite sizes calculated using the Debye–Scherrer equation. The PSA data were evaluated based on the average particle size and the Polydispersity Index (PDI) to assess particle size distribution. Finally, the results obtained from all characterization techniques were comparatively analyzed to evaluate the effect of different lemongrass and betel leaf extract ratios on the optical characteristics, particle size, and crystal structure of the synthesized silver nanoparticles.

RESULTS

1. UV–Vis Characterization

UV–Vis characterization was performed to confirm the formation of silver nanoparticles based on the appearance of the Surface Plasmon Resonance (SPR) absorption band. Measurements were conducted within the wavelength range of 398 – 450 nm using a UV–Vis spectrophotometer. The results showed that each extract ratio produced a distinct absorption peak. The UV–Vis spectra are presented in Figure 1.

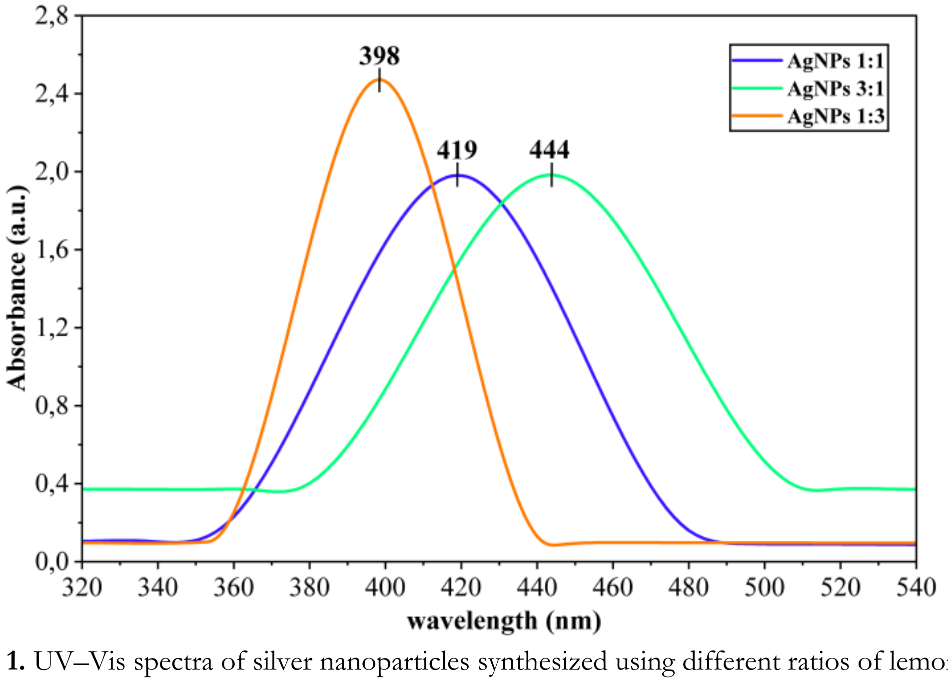

Figure 1. UV–Vis spectra of silver nanoparticles synthesized using different ratios of lemongrass and betel leaf extracts.

Based on the UV–Vis spectra, all extract ratio variations exhibited characteristic SPR bands, confirming the successful formation of silver nanoparticles. The 1:1 ratio showed a maximum absorption wavelength of 419 nm with an absorbance value of 1.98. The 3:1 ratio exhibited a maximum wavelength of 444 nm with an absorbance of 1.98, whereas the 1:3 ratio displayed an absorption peak at 398 nm with the highest absorbance value of 2.47.

To provide a clearer comparison of the UV–Vis characterization results, the maximum absorption wavelengths and absorbance values for each extract ratio are summarized in Table 1.

Table 1. Maximum absorption wavelength obtained from UV–Vis characterization

Extract Ratio	Maximum Wavelength (nm)	Absorbance
1:1	419	1.98
3:1	444	1.98
1:3	398	2.47

Table 1 demonstrates that variations in the extract ratio influenced both the maximum absorption wavelength and the absorbance intensity of the synthesized silver nanoparticles. These differences in optical characteristics indicate that the composition of the bioreducing agents affects the synthesis process and optical properties of AgNPs.

2. X-Ray Diffraction (XRD) Characterization

X-Ray Diffraction (XRD) characterization was conducted to identify the crystal structure of the synthesized silver nanoparticles and to determine their crystallite size using the Debye–Scherrer equation. The diffraction patterns of all samples are presented in Figure 2.

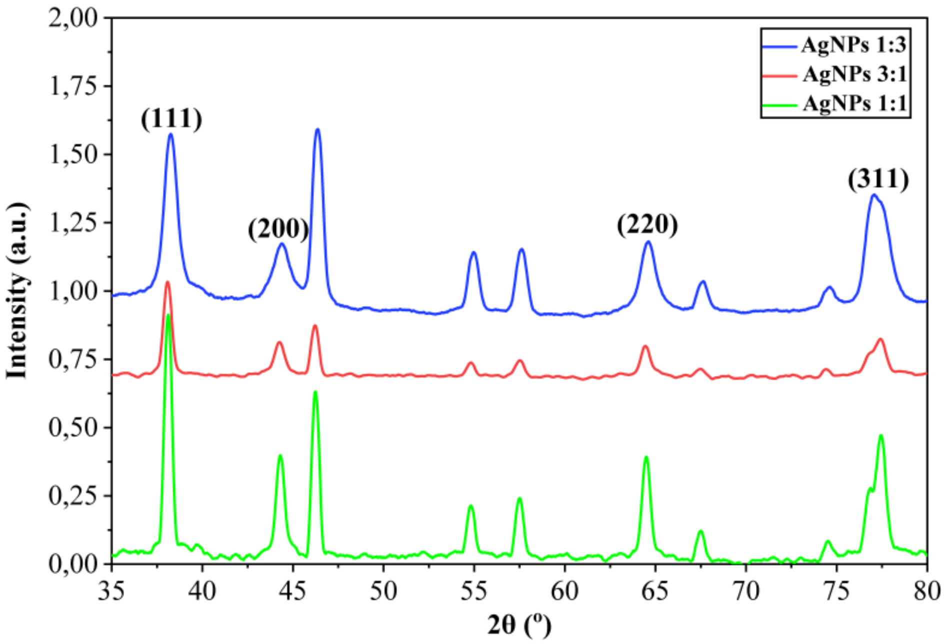

Figure 2. XRD diffraction patterns of green-synthesized silver nanoparticles prepared using different lemongrass and betel leaf extract ratios (1:1, 3:1, and 1:3).

The diffraction patterns of all samples exhibited four major diffraction peaks corresponding to the (111), (200), (220), and (311) crystal planes, confirming the characteristic Face-Centered Cubic (FCC) crystal structure of silver nanoparticles.

The crystallite size was calculated using the Full Width at Half Maximum (FWHM) values of each diffraction peak. The crystallite sizes obtained from the (111) plane were 17.80 nm, 16.47 nm, and 10.48 nm for the 1:1, 3:1, and 1:3 extract ratios, respectively. Calculations based on the other diffraction planes also revealed variations in crystallite size resulting from changes in the extract ratio.

The detailed XRD analysis results are presented in Table 2**.**

Table 2. XRD analysis results of silver nanoparticles

Crystal Plane (Bidang hkl)	Rasio 1:1			Rasio 3:1			Rasio 1:3		
	2θ (°)	B (°)	d (nm)	2θ (°)	B (°)	d (nm)	2θ (°)	B (°)	d (nm)
(111)	38.11	0.47246	17.80	38.08	0.513	16.47	38.25	0.8028	10.48
(200)	44.30	0.51575	17.20	44.26	0.605	14.24	44.40	0.88043	9.78
(220)	64.48	0.51654	18.21	64.45	0.568	16.55	64.62	0.90576	10.38
(311)	77.42	0.74547	13.66	77.42	0.881	11.61	77.08	1.48455	6.84

As shown in Table 2, XRD characterization confirmed that all synthesized samples possessed a Face-Centered Cubic (FCC) crystal structure. Moreover, variations in the extract ratio affected the FWHM values and consequently influenced the calculated crystallite size.

3. Particle Size Analyzer (PSA) Characterization

Particle Size Analyzer (PSA) characterization was performed to determine the average particle size of the green-synthesized silver nanoparticles. The particle size distributions for each extract ratio are presented in Figure 3**.**

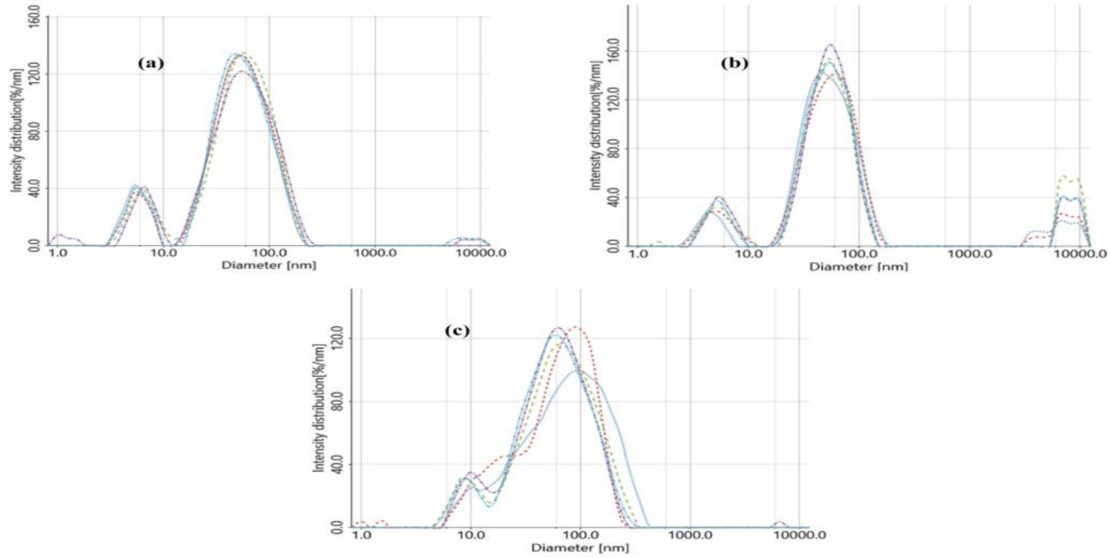

Figure 3. Particle size distribution of silver nanoparticles determined by PSA analysis.

The PSA measurements showed that the average particle size differed among the extract ratio variations. The 1:1 ratio produced the smallest average particle size of 39.1 ± 0.9 nm with a Polydispersity Index (PDI) of 0.313 ± 0.001, indicating a relatively homogeneous particle size distribution. The 3:1 ratio produced the largest average particle size of 59.7 ± 16.1 nm, whereas the 1:3 ratio resulted in an average particle size of 47.2 ± 4.6 nm. The PSA characterization results are summarized in Table 3**.**

Table 3. PSA characterization results of silver nanoparticles

Bioreducer Ratio	Particle Size (nm)	PDI
1:1	39.1 ± 0.9	0.313 ± 0.001
3:1	59.7 ± 16.1	0.138 ± 0.075
1:3	47.2 ± 4.6	0.311 ± 0.009

Note: Data are presented as mean ± standard deviation (n = 5).

Based on the PSA results presented in Table 3, the average particle sizes of all synthesized silver nanoparticles were within the nanometer scale. Furthermore, the obtained Polydispersity Index (PDI) values indicate differences in the uniformity of particle size distribution among the different extract ratio variations.

DISCUSSION

1. UV–Vis Characterization

UV–Vis spectroscopic characterization was performed to confirm the formation of silver nanoparticles through the appearance of the Surface Plasmon Resonance (SPR) absorption band. The SPR phenomenon represents the collective oscillation of free electrons on the surface of metallic nanoparticles when interacting with electromagnetic radiation at specific wavelengths. For AgNPs, the SPR absorption band generally appears within the wavelength range of 400–450 nm, although its position may shift depending on particle size and morphology, the degree of aggregation, the refractive index of the surrounding medium, and the biomolecules adsorbed on the nanoparticle surface (Fahim et al., 2024; Latumakulita, 2022; Vanlalveni et al., 2021).

The results demonstrated that variations in the lemongrass and betel leaf extract ratios influenced the optical characteristics of the synthesized AgNPs. The 1:1 ratio produced an SPR peak at 419 nm with an absorbance of 1.98, the 3:1 ratio exhibited a maximum peak at 444 nm with an absorbance of 1.98, whereas the 1:3 ratio produced an SPR peak at 398 nm with the highest absorbance value of 2.47. The differences in peak position and absorbance intensity indicate that changes in extract composition affected the nanoparticle formation process. Although the 1:3 ratio exhibited a slight blue shift, all observed wavelengths (398–444 nm) remained within the characteristic SPR region of silver nanoparticles.

The shift of the SPR band toward a shorter wavelength (blue shift) observed for the 1:3 ratio suggests changes in the optical characteristics associated with nanoparticle size or surface conditions resulting from interactions between plant-derived biomolecules and the nanoparticle surface. In contrast, the 3:1 ratio exhibited a red shift to 444 nm, indicating relatively larger particle growth or an increased tendency toward particle aggregation. These findings suggest that the composition of the bioreducing agents significantly influences the nucleation and growth processes during nanoparticle synthesis.

The highest absorbance value obtained for the 1:3 ratio (2.47) indicates that this suspension exhibited the strongest optical interaction with incident light at the SPR wavelength. However, a higher absorbance does not necessarily indicate smaller particle size because absorbance is influenced by nanoparticle concentration, particle size, morphology, and surface characteristics. Therefore, the UV–Vis results should be confirmed through X-

Ray Diffraction (XRD) analysis to determine the crystal structure, followed by Particle Size Analyzer (PSA) measurements to evaluate the hydrodynamic particle size.

The observed differences in optical characteristics are likely associated with variations in the concentrations of secondary metabolites, including flavonoids, phenolic compounds, citral, eugenol, hydroxychavicol, and tannins, which function as both reducing and stabilizing agents. Changes in extract composition alter the balance between the reduction of Ag^{+} ions into Ag^{0} and nanoparticle growth, thereby producing different optical characteristics. These findings are consistent with previous studies (Diab et al., 2025; Karaiyagowder et al., 2023; Kurra, Velidandi, Sarvepalli, & Godishala, 2025), which reported that plant extract composition significantly affects the SPR peak position and absorbance intensity of AgNPs.

2. X-Ray Diffraction (XRD) Characterization

X-Ray Diffraction (XRD) characterization was carried out to identify the crystalline phase and determine the crystallite size of the green-synthesized silver nanoparticles. Figure 4 presents the XRD diffraction patterns of AgNPs synthesized using three different lemongrass and betel leaf extract ratios (1:1, 3:1, and 1:3). All diffraction patterns exhibited four characteristic peaks located at approximately $2\theta = 38.11°$, $44.29°$, $64.44°$, and $77.40°$, corresponding to the (111), (200), (220), and (311) crystallographic planes, respectively. These diffraction peaks confirmed the formation of the characteristic Face-Centered Cubic (FCC) crystal structure of metallic silver, indicating that green synthesis using the combined lemongrass and betel leaf extracts successfully produced crystalline AgNPs without the formation of dominant impurity phases. These results are in agreement with previous reports (Karaiyagowder et al., 2023; Kurra, Velidandi, Sarvepalli, Pabbathi, et al., 2025; Rakib-Uz-Zaman et al., 2022).

The XRD results further supported the UV–Vis characterization, which had already indicated the formation of silver nanoparticles through the appearance of the SPR absorption band. While UV–Vis spectroscopy provides information regarding the optical properties of AgNPs, XRD confirms that the synthesized nanoparticles possess the characteristic Face-Centered Cubic (FCC) crystal structure of metallic silver. Although all extract ratios exhibited similar diffraction peak positions, noticeable differences in peak intensity and Full Width at Half Maximum (FWHM) values were observed, indicating variations in crystallite size resulting from differences in the composition of the bioreducing agents.

Crystallite size was calculated using the Debye–Scherrer equation based on the FWHM values. The average crystallite sizes were 16.72 nm for the 1:1 ratio, 14.72 nm for the 3:1 ratio, and 9.37 nm for the 1:3 ratio. As expected, broader diffraction peaks (higher FWHM values) corresponded to smaller crystallite sizes. Consequently, the 1:3 ratio produced the smallest crystallites, whereas the 1:1 ratio resulted in the largest crystallites.

The observed differences in crystallite size indicate that the composition of the bioreducing agents influences the nucleation and crystal growth processes during nanoparticle synthesis. Increasing the proportion of betel leaf extract in the 1:3 ratio likely supplied higher concentrations of bioactive compounds, including flavonoids, phenolic compounds, tannins, eugenol, and hydroxychavicol, thereby accelerating crystal nucleation and restricting the growth of individual crystallites. Conversely, the 1:1 ratio promoted more extensive crystal growth, resulting in larger crystallites. These findings are consistent with previous studies (Diab et al., 2025; Karaiyagowder et al., 2023; Kurra, Velidandi, Sarvepalli, Pabbathi, et al., 2025), which demonstrated that plant extract composition significantly influences the crystallite size of AgNPs.

The crystallite sizes determined by XRD were consistently smaller than the particle sizes obtained from PSA, namely 39.1 ± 0.9 nm, 59.7 ± 16.1 nm, and 47.2 ± 4.6 nm for the 1:1, 3:1, and 1:3 ratios, respectively. This difference is commonly observed because XRD measures the size of individual crystalline domains, whereas PSA determines the hydrodynamic particle size in suspension, including the surrounding biomolecular capping layer and possible particle agglomeration (Fahim et al., 2024; Raj et al., 2022).

Overall, the XRD results demonstrate that variations in the lemongrass and betel leaf extract ratios did not alter the crystalline phase of AgNPs, which consistently retained the characteristic FCC structure. However, the extract ratio significantly affected crystallite size, with the 1:3 ratio producing the smallest crystallites (9.37 nm) and the 1:1 ratio producing the largest crystallites (16.72 nm). These findings indicate that the composition of the bioreducing agents plays a critical role in controlling crystal growth during green synthesis. Although XRD successfully determined crystallite size, this parameter does not represent the overall particle size in suspension. Therefore, PSA characterization was subsequently performed.

3. Particle Size Analyzer (PSA) Characterization

Following the determination of crystal structure and crystallite size by XRD analysis, Particle Size Analyzer (PSA) characterization was performed to determine the hydrodynamic size of silver nanoparticles in suspension. Unlike the crystallite size obtained from XRD, which represents the dimensions of individual crystalline domains, PSA measures the overall particle size together with the biomolecular capping layer surrounding the nanoparticles. Consequently, PSA measurements generally produce larger particle sizes than XRD measurements. Therefore, PSA serves as a complementary technique to XRD, providing a more comprehensive evaluation of nanoparticle dimensions under colloidal conditions (Fahim et al., 2024; Latumakulita, 2022; Raj et al., 2022).

The results showed that particle size was influenced by the extract ratio. The 1:1 ratio produced the smallest average particle size (39.1 ± 0.9 nm), followed by the 1:3 ratio (47.2 ± 4.6 nm), whereas the 3:1 ratio yielded the largest particles (59.7 ± 16.1 nm). These findings indicate that a balanced composition of lemongrass and betel leaf extracts at the 1:1 ratio was more effective in controlling particle growth during the synthesis process.

The smaller particle size obtained at the 1:1 ratio suggests that a balanced concentration of secondary metabolites from both extracts promoted the formation of a larger number of nucleation sites during the initial stage of synthesis. The increased number of nuclei distributed the reduced Ag^0 atoms among more growth centers, thereby limiting particle growth and producing smaller nanoparticles. In contrast, the predominance of one extract in the 3:1 ratio likely prolonged particle growth, resulting in larger particle sizes.

Although the 1:3 ratio exhibited the highest UV–Vis absorbance, it did not produce the smallest particle size. This finding demonstrates that absorbance intensity does not necessarily correlate directly with particle size because UV–Vis absorbance is influenced by nanoparticle concentration and optical properties, whereas PSA measures the physical dimensions of particles dispersed in suspension.

The Polydispersity Index (PDI) value of 0.313 ± 0.001 obtained for the 1:1 ratio indicates a relatively homogeneous particle size distribution. In general, PDI values below 0.5 indicate a relatively narrow particle size distribution, while values approaching zero represent greater uniformity. Therefore, the 1:1 ratio produced the most homogeneous particle size distribution among the investigated extract ratios. These findings are consistent with previous studies (Diab et al., 2025; Karaiyagowder et al., 2023; Kurra, Velidandi, Sarvepalli, Pabbathi, et al., 2025), which reported that the composition of plant extracts used as bioreducing agents significantly affects nanoparticle size and colloidal stability.

Although XRD successfully identified the crystal structure and crystallite size of the synthesized nanoparticles, it does not provide information regarding the overall particle dimensions in suspension. Therefore, PSA characterization is essential for determining the hydrodynamic size of silver nanoparticles.

4. Relationship Among UV–Vis, XRD, and PSA Characterization Results

UV–Vis spectroscopy confirmed the formation of silver nanoparticles through the characteristic Surface Plasmon Resonance (SPR) absorption band. XRD subsequently verified the crystal structure and determined the crystallite size of the synthesized nanoparticles. PSA then provided information regarding the hydrodynamic particle size and particle size distribution in suspension. Together, these three complementary characterization techniques provide a comprehensive understanding of the physicochemical properties of AgNPs (Fahim et al., 2024; Latumakulita, 2022; Raj et al., 2022).

The results demonstrated that each extract ratio produced distinct nanoparticle characteristics. The 1:3 ratio yielded the highest UV–Vis absorbance (2.47) and the smallest crystallite size according to XRD analysis (9.37 nm), whereas the 1:1 ratio produced the smallest average particle size (39.1 ± 0.9 nm) together with the most homogeneous particle size distribution based on the PDI value. In contrast, the 3:1 ratio generated the largest particle size (59.7 ± 16.1 nm) and an intermediate crystallite size compared with the other two ratios.

These findings indicate that the UV–Vis, XRD, and PSA results cannot be directly compared because each technique measures different physicochemical parameters. UV–Vis spectroscopy evaluates the optical response of nanoparticles, XRD determines the size of individual crystalline domains based on diffraction peak broadening, whereas PSA measures the hydrodynamic particle size, which is influenced by the surrounding biomolecular capping layer and possible particle agglomeration. Consequently, the particle sizes obtained from PSA are generally larger than the crystallite sizes determined by XRD (Fahim et al., 2024; Raj et al., 2022).

Based on the integration of these three characterization techniques, the increased proportion of betel leaf extract in the 1:3 ratio likely promoted the formation of a greater number of crystal nuclei, thereby restricting crystallite growth and producing smaller crystallites. Conversely, the balanced composition of extracts in the 1:1 ratio more effectively controlled overall particle growth, resulting in smaller particle sizes and a more homogeneous particle size distribution. Nevertheless, all synthesized samples consistently retained the characteristic Face-Centered Cubic (FCC) crystal structure of silver nanoparticles.

Overall, the findings demonstrate that no single extract ratio was superior across all characterization parameters. The 1:3 ratio exhibited the strongest optical characteristics and the smallest crystallite size, whereas the 1:1 ratio produced the smallest particle size and the most homogeneous particle size distribution. These results indicate that variations in the ratio of lemongrass and betel leaf extracts play a crucial role in controlling the physicochemical characteristics of AgNPs synthesized via the green synthesis approach.

CONCLUSION

Silver nanoparticles (AgNPs) were successfully synthesized through a green synthesis approach using a combination of lemongrass (*Cymbopogon citratus*) and betel (*Piper betle*) leaf extracts as bioreducing agents for the $AgNO_3$ precursor. Variations in the extract ratios (1:1, 1:3, and 3:1) significantly influenced the optical characteristics, particle size, and crystallite size of the synthesized AgNPs. UV–Vis characterization confirmed the formation of AgNPs through the appearance of Surface Plasmon Resonance (SPR) absorption bands within the wavelength range of 398–444 nm, with the 1:3 extract ratio exhibiting the highest absorbance. X-Ray Diffraction (XRD) analysis further demonstrated that all synthesized samples possessed the characteristic Face-Centered Cubic (FCC) crystal structure, with the smallest crystallite size obtained at the 1:3 ratio. In contrast, Particle Size Analyzer (PSA) measurements revealed that the smallest average particle size was achieved at the 1:1 ratio. Overall, the findings indicate that the extract ratio used as the bioreducing agent plays a crucial role in controlling the physicochemical characteristics of AgNPs synthesized via the green synthesis method.

This study provides a valuable scientific contribution to the development of environmentally friendly and sustainable green synthesis methods for silver nanoparticles by utilizing a combination of two natural plant extracts, namely lemongrass and betel leaves, as bioreducing agents. The findings regarding the influence of extract ratio variations on the optical characteristics, crystallite size, and particle size of AgNPs enhance the current understanding of the role of bioreducer composition in controlling nanoparticle quality.

Furthermore, the results may serve as a scientific reference for the development of nanoparticle synthesis based on locally available biological resources and support future applications of AgNPs in functional materials, antibacterial agents, biomedical technologies, and sensing devices.

Future studies are recommended to optimize additional synthesis parameters, including solution pH, reaction temperature, incubation time, $AgNO_3$ precursor concentration, and bioreducing extract concentration, to obtain silver nanoparticles with improved size uniformity and colloidal stability. In addition, further characterization using techniques such as Transmission Electron Microscopy (TEM), Scanning Electron Microscopy (SEM), Fourier Transform Infrared Spectroscopy (FTIR), and zeta potential analysis is recommended to provide more comprehensive information regarding nanoparticle morphology, surface functional groups, and colloidal stability. Evaluation of biological activities, including antibacterial, antioxidant, and cytotoxic properties, should also be conducted to further assess the application potential of green-synthesized silver nanoparticles in healthcare, environmental remediation, and advanced materials technology.

REFERENCES

Cherian, T., Ali, K., & Musarrat, J. (2025). Green functionalization of silver nanoparticles using leaf extract of *Cymbopogon citratus* and assessment of their biological activities. *Next Nanotechnology, 8*, 100216. https://doi.org/10.1016/j.nxnano.2025.100216

Diab, M., Jadhav, A. H., & Alwarsamy, M. (2025). The synergistic effect of biosynthesized silver nanoparticles from a combined extract of *Petroselinum crispum* and *Piper betle*: In vitro antibacterial activity. *Results in Chemistry, 18*, 102816. https://doi.org/10.1016/j.rechem.2025.102816

Fahim, M., Shahzaib, A., Nishat, N., Jahan, A., Bhat, T. A., & Inam, A. (2024). Green synthesis of silver nanoparticles: A comprehensive review of methods, influencing factors, and applications. *JCIS Open, 16*, 100125. https://doi.org/10.1016/j.jciso.2024.100125

Govindarajan, D. K., Selvaraj, V., Selvaraj, A. S. J. M., Hameed, S. S., Pandiarajan, J., & Veluswamy, A. (2023). Green synthesis of silver micro- and nanoparticles using phytochemical extracts of *Cymbopogon citratus* exhibits antibacterial properties. *Materials Today: Proceedings, 76*, 103–108. https://doi.org/10.1016/j.matpr.2022.10.133

Kumari, S., & Sarkar, L. (2021). A review on nanoparticles: Structure, classification, synthesis & applications. *Journal of Scientific Research, 65*(8), 42–46. https://doi.org/10.37398/JSR.2021.650809

Kurra, H., Velidandi, A., Sarvepalli, M., & Godishala, V. (2025). Green-synthesized silver nanoparticles from *Cymbopogon citratus*: Synergistic antibacterial effects and food safety potential. *Journal of Food Chemistry and Nanotechnology, 11*(1), 15–24. https://doi.org/10.17756/jfcn.2025-198

Kurra, H., Velidandi, A., Sarvepalli, M., Pabbathi, N. P. P., & Godishala, V. (2025). Aqueous *Cymbopogon citratus* extract-mediated silver nanoparticles: Part I. Influence of synthesis parameters, characterization, and biomedical studies. *Nanomaterials, 15*(5), 328. https://doi.org/10.3390/nano15050328

Latumakulita, I. I., & Suparno. (2022). Characterization of silver nanoparticle electrolysis method with UV-Vis spectrometer, atomic absorption spectrophotometer, and particle size analyzer. *Kasuari: Physics Education Journal, 5*(1), 42–52. https://doi.org/10.37891/kpej.v5i1.178

Moond, M., Singh, S., Sangwan, S., Devi, R., & Beniwal, R. (2022). Green synthesis and applications of silver nanoparticles: A systematic review. *AATCC Journal of Research, 9*(6), 272–285. https://doi.org/10.1177/24723444221119847

Mustapha, T., Misni, N., Ithnin, N. R., Daskum, A. M., & Unyah, N. Z. (2022). A review on plants and microorganisms mediated synthesis of silver nanoparticles, role of plants metabolites and applications. *International Journal of Environmental Research and Public Health, 19*(2), 674. https://doi.org/10.3390/ijerph19020674

Pandey, P., Lakhanpal, S., Bishoyi, A. K., Jyothi, S. R., Mishra, S., Verma, M., Singh, A., Alam, M. W., Rab, S. O., Saeed, M., & Khan, F. (2025). Biosynthesis of silver nanoparticles from plant extracts: A comprehensive review focused on anticancer therapy. *Frontiers in Pharmacology, 16*, 1600347. https://doi.org/10.3389/fphar.2025.1600347

Raj, S., Trivedi, R., & Soni, V. (2022). Biogenic synthesis of silver nanoparticles, characterization and their applications—A review. *Surfaces, 5*(1), 67–90. https://doi.org/10.3390/surfaces5010003

Rakib-Uz-Zaman, S. M., Hoque Apu, E., Muntasir, M. N., Mowna, S. A., Khanom, M. G., Jahan, S. S., Akter, N., R. Khan, M. A., Shuborna, N. S., Shams, S. M., & Khan, K. (2022). Biosynthesis of silver nanoparticles from *Cymbopogon citratus* leaf extract and evaluation of their antimicrobial properties. *Challenges, 13*(1), 18. https://doi.org/10.3390/challe13010018

Rónavári, A., Igaz, N., Adamecz, D. I., Szerencsés, B., Molnar, C., Kónya, Z., Pfeiffer, I., & Kiricsi, M. (2021). Green silver and gold nanoparticles: Biological synthesis approaches and potentials for biomedical applications. *Molecules, 26*(4), 844. https://doi.org/10.3390/molecules26040844

Sampath, G., Chen, Y.-Y., Rameshkumar, N., Krishnan, M., Nagarajan, K., & Shyu, D. J. H. (2022). Biologically synthesized silver nanoparticles and their diverse applications. *Nanomaterials, 12*(18), 3126. https://doi.org/10.3390/nano12183126

Vanlalveni, C., Lallianrawna, S., Biswas, A., Selvaraj, M., Changmai, B., & Rokhum, S. L. (2021). Green synthesis of silver nanoparticles using plant extracts and their antimicrobial activities: A review of recent literature. *RSC Advances, 11*(5), 2804–2837. https://doi.org/10.1039/D0RA09941D